

Technical Note

Cite this article: Chiang B-H, Chen Y, MacDurmon G, and Ahmad S. (2021) Quantitative assessment of the production of radioactive materials by the Mevion S250i Hyperscan proton therapy system: a year-long survey. *Journal of Radiotherapy in Practice* 20: 361–364. doi: [10.1017/S1460396920000515](https://doi.org/10.1017/S1460396920000515)

Received: 8 May 2020
Revised: 1 June 2020
Accepted: 5 June 2020
First published online: 8 July 2020


Key words:

Mevion S250i Hyperscan; proton therapy; radioactive materials; room survey

Author for correspondence:

Bing-Hao Chiang, Department of Radiation Oncology, Peggy and Charles Stephenson Cancer Center, University of Oklahoma Health Sciences Center, Oklahoma City, OK, USA.
E-mail: binghao-chiang@ouhsc.edu

Quantitative assessment of the production of radioactive materials by the Mevion S250i Hyperscan proton therapy system: a year-long survey

Bing-Hao Chiang , Yong Chen, George MacDurmon and Salahuddin Ahmad

Department of Radiation Oncology, Peggy and Charles Stephenson Cancer Center, University of Oklahoma Health Sciences Center, Oklahoma City, OK, USA

Abstract

Introduction: This technical note describes a quantitative assessment of the production of radioactive materials during a year-long clinical operation of a Mevion S250i Hyperscan proton therapy system. The production of accumulated radioactive materials plays an important role in determining radiation safety in and around the proton therapy facilities.

Methods: We have conducted a weekly room survey, every week for a year, during normal clinical operation.

Results and conclusions: We estimated the accumulated activity from secondary neutron activation on aluminium structures at 3 m away from isocentre in the beamline to be less than 300 μCi .

Introduction

Proton therapy shows the ability of reducing normal tissue doses while maintaining adequate dose coverage to tumour for many different sites.^{1–4} Two beam delivery techniques were generally used in proton therapy, which include passively scattered proton therapy (PSPT) and scanning beam proton therapy (SBPT).⁵ The PSPT utilises a single or double scattering foil/foils to spread the beam and achieve lateral beam coverage, while SBPT such as uniform scanning and pencil beam scanning (PBS) proton therapy involves directly moving a pencil shape-charged particle beam (here in this case proton) while depositing the dose throughout the target volume. The MEVION S250i with HYPERSCAN and Adaptive Aperture™ (Mevion Medical Systems Inc., Littleton, MA, USA) is a single room compact PBS system, recently installed and commissioned only in few institutions. This compact design utilising a gantry-mounted superconducting synchrocyclotron eliminates the need for complex beam transport system and provides lower cost option for implementing proton therapy. Comparing with the PSPT nozzle, the PBS nozzle does not need any scattering foils in the beamline. Patient-specific apertures were also eliminated and a new Adaptive Aperture (AA) system was introduced to collimate the peripheral proton spots. Patient compensator was also replaced by the range shifter plates to modify the beam energy and depths. A TOPAS Monte Carlo simulation of such system shown detailed system schematic in Figure 1.⁶

The production of radioactive materials plays an important role in radiation safety for proton therapy facilities.⁷ A quantitative assessment of the production of long-live radioactive materials is also required for state licensing and radiation safety assessment. In our case, radioactive materials are mainly produced as a result of the operation of the synchrocyclotron accelerator. Cyclotron components, beam transport line and other room structure elements become radioactive due to the direct irradiations with proton beam as well as indirect irradiations with secondary particles. The main objective of the present study has been to provide a quantitatively assessment of the production of radioactive materials during a year-long clinical operation of a Mevion S250i Hyperscan proton therapy system. To the best of our knowledge, this report is the first of its kind to address residual radioactivity from a clinical-operated particle therapy system.

Materials and Methods

Radioactive material production

The possible source terms for the Mevion S250i Hyperscan proton system may include the following: (1) activation of cyclotron due to internal beam loss, (2) activation of collimating components after beam exit, (3) activation of carbon used as absorber material after beam exit, (4) activation of aluminium used in the frames and supports near the beamline, (5) activation of accelerator and vault by thermal neutron capture secondary to proton beam irradiation and

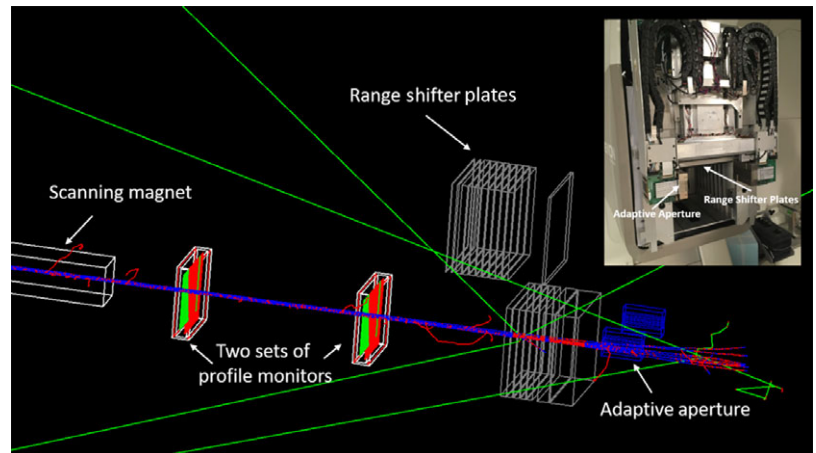


Figure 1. TOPAS Monte Carlo simulation schematic of Mevion S250i HYPERSCAN nozzle.

(6) activation of air and water in the vault by high-energy protons. The activation of cyclotron will be consistent with those produced in high-energy accelerator when high-energy proton interactions on steel and brass components. The expected isotopes are principally including Be-7, C-11, F-18, Na-22, Na-24, Sc-46, Sc-48, V-48, Cr-51, Mn-52, Mn-54, Co-57, Co-60 and Zn-65. After the proton beam entering nozzle, the activation of collimating components might also happen when the proton is stopping by the AA, which is made of brass. The possible isotopes would be similar to those activations at cyclotron as listed above. The proton beam will also interact with carbon-based absorber material in range shifter plates and produce radioactive isotope. The products of proton interactions on carbon could be H-3, Be-7, C10 and C-11. Tritium, with half-life of 12.3 years, will not reach quantities in the μCi range.

On the other hand, the principal materials, such as copper and manganese, near an accelerator with significant thermal neutron activation cross-section will interact with secondary neutron too. The principal produced isotopes include Cu-64 and Mn-56. Eu-152 can also be produced by the neutron capture reaction in trace amounts of stable Europium of concrete.⁸ The aluminium used in frame and supports near the beamline might also become activated by spallation reaction with secondary neutrons above 20 MeV. Activation products of spallation reaction are limited to F-18, Na-24 and Na-22. For last possible source, the radioactive isotopes with short half-life such as O-14, O-15, N-13 and C-11 will also be produced when high-energy beam passes through air or water.

Among all possible radioactive nuclides, Na-22 from spallation reaction and neutron captured produced Eu-152 with long half-life of 2.6 and 13.54 years were assumed to be the main contributor in this assessment; other possible radionuclide can also be found but Eu-152 and Na-22 are the most important.⁹ Therefore, in this technical note, the accumulated activity of Na-22 and Eu-152 will be calculated based on the measured dose level at isocentre.

Year-long weekly room survey

To qualitatively assess the production of radioactive materials during the normal condition of clinical operation, we have conducted a year-long weekly room survey starting from 28 January 2019. The residual radioactive level was monitored inside the treatment room on every Sunday morning after roughly 40 hours of normal daily operation of patient treatments which ended around 5 PM Friday afternoon. Three locations of measurement that included room corner, room isocentre and nozzle surface are shown in Figure 2. A hand-held gamma spectrometer, identiFINDER-U (Thermo Scientific, Waltham, MA, USA) was used for the room

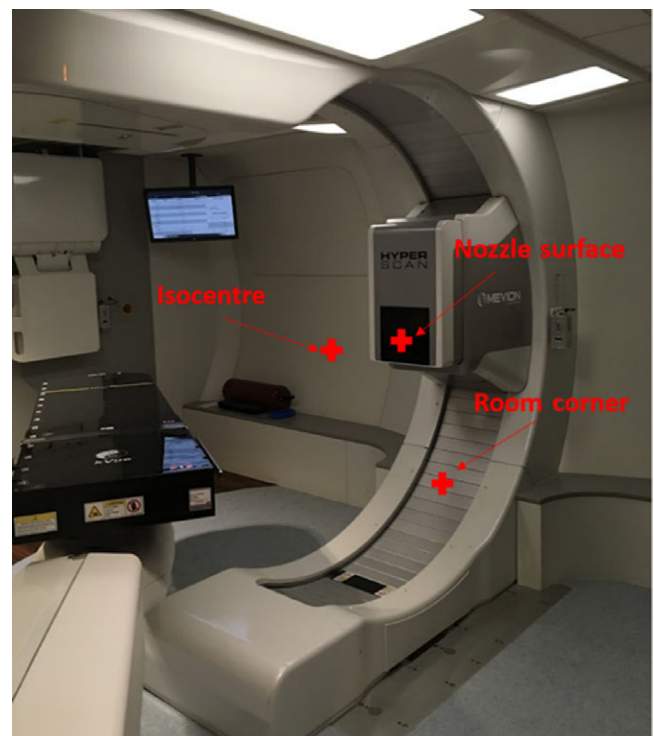


Figure 2. Scheme of measurement points at treatment room of MEVION S250i proton therapy system.

survey for the production of accumulated radioactive materials during normal clinical operation.

Relationship between radionuclide gamma emission and exposure rate

The relationship between exposure (X) and energy fluence (Ψ) can be obtained by the following equation:

$$X = \Psi \left(\frac{\mu_{en}}{\rho} \right)_{air} \left(\frac{e}{\overline{W}} \right)_{air} \quad (1)$$

where $\left(\frac{\mu_{en}}{\rho} \right)_{air}$ and $\left(\frac{\overline{W}}{e} \right)_{air}$ are the mass energy absorption coefficients and the average energy required per unit charge of ionisation produced in air, respectively.

Table 1. The decay information of Na-22 including energies, yields and mass attenuation coefficients

Energy (MeV)	Yield (%)	$(\frac{\mu_{en}}{\rho})_{air}$ (cm ² /g)
0-000848	0-0535	4-33 E + 03
0-000849	0-107	4-33 E + 03
1-274537	99-94	2-65 E-02
0-511	180-76	2-96 E-02

Table 2. The decay information of Eu-152 including energies, yields and mass attenuation coefficients

Energy (MeV)	Yield (%)	$(\frac{\mu_{en}}{\rho})_{air}$ (cm ² /g)	Energy (MeV)	Yield (%)	$(\frac{\mu_{en}}{\rho})_{air}$ (cm ² /g)
0-08985	69-7	2-37 E-02	0-045414	7-2616	0-05352271
0-040118	37-78	6-80 E-02	0-121773	7-08	0-02399464
0-121782	28-53	2-40 E-02	0-040902	6-4915	0-06586303
0-344279	26-592	2-91 E-02	0-00564	4-75	28-6796
0-00585	25-819	25-1915	0-86738	4-233	0-02850668
0-039522	21-05	0-07241069	0-045293	3-758	0-05385365
1-408013	20-879	0-02590786	0-86738	4-23	0-02850668
0-964057	14-517	0-02805713	0-045293	3-758	0-05385365
0-841634	14-216	0-0286264	0-443961	2-827	0-02956473
0-00564	14-05	28-6796	0-045414	2-53	0-05352271
1-112076	13-678	0-02733859	0-046578	2-405	0-05033917
0-040118	13-217	0-06800727	0-344293	2-44	0-02906106
0-778905	12-938	0-02889489	0-047038	2-255	0-04908107
0-963384	11-613	0-02806026	0-411117	2-23713	0-0295089
0-041542	11-63	0-06411263	1-299142	1-633	0-02642608
1-085837	10-115	0-02746768	0-045293	1-32	0-05385365
0-244698	7-554	0-02761395	0-046905	1-163	0-04944483
0-039522	7-39	0-07241069			

The energy fluence rate (Ψ) from a radioactive source can be determined by the following equation:

$$\Psi = \frac{AyE}{4\pi r^2} \tag{2}$$

where ‘A’ represents the activity of the source in becquerels (Bq), ‘y’ and ‘E’ represent the yield and energy of photons, respectively and ‘r’ is the distance in cm.

Using the above two equations, we then obtained the relationships between the exposure rate (\dot{X}) and radionuclide gamma emission by the following equation:

$$\dot{X} = \frac{AyE}{4\pi r^2} \left(\frac{\mu_{en}}{\rho}\right)_{air} \left(\frac{e}{W}\right)_{air} \tag{3}$$

Using an average of 33-8 eV per ion pair, combining all the numerical terms, and considering gamma ray in different energies and yields, we obtained the following:

$$\dot{X} = 5.263 \times 10^{-6} A \sum \frac{y_i E_i \left(\frac{\mu_{en}}{\rho}\right)_i}{r^2} \tag{4}$$

where A is in Bq, y_i and E_i represent the yield and energy of photon at each energy i (MeV). The decay information of Na-22 and Eu-152 including energies, yields and mass attenuation coefficients is shown in Tables 1 and 2, respectively.^{10,11}

Results and Discussion

The year-long measurements for the locations of room isocentre and the corner are shown in Figure 3. The room activation levels were shown to gradually increase in the first 9 months and slowly plateaued thereafter. A few outlier data point readings were highlighted as they were taken during insufficient machine cold down time due to weekend patient treatment and maintenance work and were removed from further analysis. From these data, we could safely assume an average activation level of 35 urem/hour at room isocentre with normal treatment operation.

The production of radioactive materials is mainly due to the neutron capture, which produces Eu-152, and spallation reaction, which generates Na-22. The typical spectrum and possible radionuclides measured from our weekly room survey at nozzle surface are shown in Figure 4.

If we assume that the measured dose level was contributed mainly by Na-22 from secondary neutron-activated structural aluminium at 3 m away from the isocentre in the beamline, then the accumulated activity of Na-22 was calculated to be 274-9 μ Ci. On the other hand, if we assume that the measured dose level was contributed mainly by Eu-152 from neutron capture of concrete at about 2 m away from isocentre, then the accumulated activity of Eu-152 was calculated to be 75-1 μ Ci. The details of our calculation are shown in the Appendix.

In this study, we conservatively assumed that the contribution of measured dose level was only from one source, namely Na-22 or Eu-152. The accumulated activity might be lower for individual radionuclide if contributions from all other possible radionuclides are considered. However, comparing two main contribution radionuclides, the accumulated activity should be less than 300 μ Ci for all possible radionuclide for the assessment purpose of the production of radioactive materials.

Conclusions

At a worst-case scenario, the accumulated activity on aluminium structures was found to be less than 300 μ Ci after 1 year of patient treatment. We do not anticipate that the accumulated radiation level would rise in the future under normal condition of operation with patient treatments. We have thus reported for the first time the residual radioactivity from a clinical operation of a compact proton therapy system. We do not anticipate the accumulated radiation level to rise in future, and safe clinical operation will thus continue.

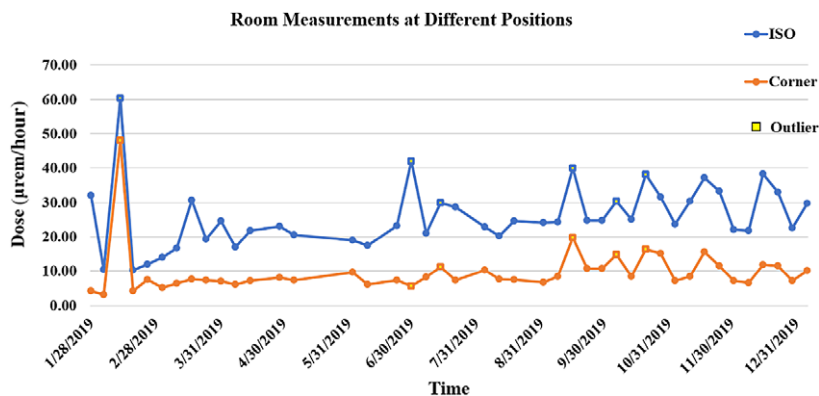


Figure 3. Year-long room survey measurements at two different locations, the outlier data points were highlight and removed from the results.

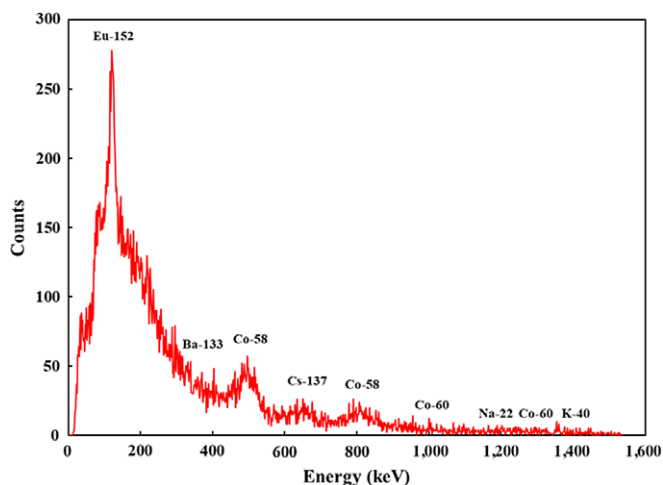


Figure 4. Energy spectrum measured at nozzle surface.

Acknowledgement. None.

References

- Boehling N S, Grosshans D R, Bluett J B et al. Dosimetric comparison of three-dimensional conformal proton radiotherapy, intensity-modulated proton therapy, and intensity-modulated radiotherapy for treatment of pediatric craniopharyngiomas. *Int J Radiat Oncol Biol Phys* 2012; 82: 643–652.
- Mock U, Georg D, Bogner J, Auberger T and Pötter R Treatment planning comparison of conventional, 3D conformal, and intensity-modulated photon (IMRT) and proton therapy for paranasal sinus carcinoma. *Int J Radiat Oncol Biol Phys* 2004; 58: 147–154.
- Vargas C, Fryer A, Mahajan C et al. Dose–volume comparison of proton therapy and intensity-modulated radiotherapy for prostate cancer. *Int J Radiat Oncol Biol Phys* 2008; 70: 744–751.
- Yock T, Schneider R, Friedmann A, Adams J, Fullerton B and Tarbell N Proton radiotherapy for orbital rhabdomyosarcoma: clinical outcome and a dosimetric comparison with photons. *Int J Radiat Oncol Biol Phys* 2005; 63: 1161–1168.
- Paganetti H Proton therapy physics. Boca Raton, Florida, USA. CRC press 2018.
- Chiang B-H, Bunker A, Jin H, Ahmad S and Chen Y. Developing a Monte Carlo model for MEVION S250i with HYPERSCAN and Adaptive Aperture™ pencil beam scanning proton therapy system. *J Radiother Prac* 2020; 1–8. doi: [10.1017/S1460396920000266](https://doi.org/10.1017/S1460396920000266)

- Moritz L E. Radiation protection at low energy proton accelerators. *Radiat Prot Dosimetry* 2001; 96: 297–309.
- Carroll L. Predicting long-lived, neutron-induced activation of concrete in a cyclotron vault. *AIP Conference Proceedings*. American Institute of Physics 2001: 301–304.
- Tesse R, Boogert S, Gnacadja E et al. Simulations of the Activation of a Proton Therapy Facility Using a Complete Beamline Model With BDSIM. 10th Int Particle Accelerator Conf(IPAC'19), Melbourne, Australia, 19–24 May 2019. JACOW Publishing, Geneva, Switzerland 2019: 4176–4179.
- National Nuclear Data website established by Brookhaven National Laboratory. https://www.nndc.bnl.gov/nudat2/indx_dec.jsp. Accessed on 4th May 2020.
- National Institution of Standard and Technology. <https://physics.nist.gov/PhysRefData/XrayMassCoef/ComTab/air.html>. Accessed on 4th May 2020.

Appendix

The relationship between radionuclide gamma emission and exposure rate is already shown in equation 4.

The decay radiation data including gamma energies and yields of decays can be found from National Nuclear Data website established by Brookhaven National Laboratory (https://www.nndc.bnl.gov/nudat2/indx_dec.jsp). The mass energy absorption coefficients for the photon in air can be obtained by interpolation from the table of National Institution of Standard and Technology (<https://physics.nist.gov/PhysRefData/XrayMassCoef/ComTab/air.html>).

The energies and yields of four possible decay photons and their mass energy absorption coefficients from parent nucleus Na-22 were listed in Table 1. Therefore, if we assume that the measured dose level was contributed mainly by Na-22 at 3 m away, the accumulated activity of Na-22 can be calculated to be 274.9 µCi using equation 5 shown below.

$$A(Ci) = \frac{\dot{X}(R/hr)}{5.263 \times 10^{-6} \sum \left(\frac{y_i E_i \left(\frac{\mu_{en}}{\rho} \right)_i}{r^2} \right)} \times \frac{1}{3.7 \times 10^{10}} \left(\frac{Ci}{Bq} \right) \quad (5)$$

The energies (above 1 MeV) and yields of four possible decay photons and their mass energy absorption coefficients from parent nucleus Eu-152 were listed in Table 2. Again, if we assume that the measured dose level was contributed mainly by Eu-152 at 2 m away from isocentre in the beamline, the accumulated activity of Eu-152 can be calculated to be 75.1 µCi using equation 5 shown above.